Biogeosciences Discuss., 6, 5549–5588, 2009
www.biogeosciences-discuss.net/6/5549/2009/

Biogeosciences Discussions

Biogeosciences Discussions is the access reviewed discussion forum of *Biogeosciences*

Reconstructing the Nd oceanic cycle using a coupled dynamical – biogeochemical model

T. Arsouze[1,2,*], J.-C. Dutay[1], F. Lacan[2], and C. Jeandel[2]

[1]Laboratoire des Sciences du Climat et de l'Environnement (LSCE), IPSL, CEA/UVSQ/CNRS, Orme des Merisiers, Gif-Sur-Yvette, Bat 712, 91191 Gif sur Yvette cedex, France
[2]Laboratoire d'Etudes en Géophysique et Océanographie Spatiale (LEGOS), UPS/CNES/CNRS/ IRD, Observatoire Midi-Pyrénées, 14 av. E. Belin, 31400 Toulouse, France
[*]now at: Lamont-Doherty Earth Observatory (LDEO), P.O. Box 1000 61 Route 9W, Palisades, NY 10964-1000, USA

Received: 11 May 2009 – Accepted: 19 May 2009 – Published: 10 June 2009

Correspondence to: T. Arsouze (arsouze@ldeo.columbia.edu)

Published by Copernicus Publications on behalf of the European Geosciences Union.

Abstract

The decoupling of behaviour observed between Nd isotopic composition (Nd IC, also referred as ε_{Nd}) and Nd concentration has led to the notion of a "Nd paradox". While ε_{Nd} behaves in a quasi-conservative way in the open ocean, leading to its broad use as a water-mass tracer, Nd concentration displays vertical profiles that increase with depth together with a deep water enrichment along the global thermohaline circulation, non-conservative behaviour typical of nutrients affected by scavenging in surface waters and remineralisation at depth. In addition, recent studies suggested that the only way to reconcile both concentration and Nd IC oceanic budgets, is to invoke a "Boundary Exchange" process (BE, defined as the co-occurrence of transfer of elements from the margin to the sea with removal of elements from the sea by Boundary Scavenging) as a source-sink term. However, these studies did not simulates the real input/output fluxes of Nd to the ocean, and therefore did prevent from crucial information to apprehend the "Nd paradox". In this study, we investigate this paradox on a global scale using for the first time a fully prognostic coupled dynamical/biogeochemical model and an explicit representation of the sources and sinks to simulate the Nd oceanic cycle. Sources considered are dissolved river fluxes, atmospheric dusts and margin sediment re-dissolution. Sinks are scavenging by settling particles. This model satisfyingly simulate the global Nd oceanic cycle, and produces realistic distribution of Nd concentration and isotopic composition, though a slight overestimation of Nd concentrations in the deep Pacific Ocean, likely revealing an underestimation of the particle fields by the biogeochemical model. Our results underlines that 1) vertical cycling (scavenging/remineralisation) is absolutely necessary to satisfyingly simulate both concentration and ε_{Nd}, and 2) BE is the dominant Nd source to the ocean. The estimated BE flux (1.1×10^{10} g(Nd)/yr) is much higher than both dissolved river discharge (2.6×10^{8} g(Nd)/yr) and atmospheric inputs (1.0×10^{8} g(Nd)/yr) that play negligible role in the water column but are necessary to reconcile Nd IC in surface and subsurface. This leads to a recalculated residence time of Nd in the ocean of 360 yrs. The BE flux

BGD

6, 5549–5588, 2009

requires the dissolution of only 3 to 5% of the annually flux of material weathered on the continent and deposited via the solid river discharge on the continental margin.

1 Introduction

Neodymium isotopic composition (hereafter referred as Nd IC[1]) variations observed within the ocean reflect both influences of lithogenic inputs of the element (whose IC varies as function of age and geological composition of the continent, Jeandel et al., 2007) and the subsequent redistribution by the oceanic circulation. ε_{Nd} data show that these variations are closely linked to water mass distribution at depth, and that far from any continental sources, Nd IC behaves quasi-conservatively (Piepgras and Wasserburg, 1982; Jeandel, 1993; von Blanckenburg, 1999; Goldstein and Hemming, 2003). Hence, the main water masses display characteristic ε_{Nd} values (e.g. NADW: $\varepsilon_{Nd} \approx -13.5$, AAIW and AABW: $\varepsilon_{Nd} \approx -8$). This water mass tracer property has been widely explored in the modern ocean, by measuring dissolved Nd IC and concentrations (Jeandel, 1993; Piepgras and Wasserburg, 1980, 1982, 1987; Shimizu et al., 1994; Lacan 2004), but has also been for reconstructing past ocean circulation from measurements in the authigenic fraction of the sediments (Rutberg et al., 2000; Piotrowski et al., 2004, 2005; Gutjahr et al., 2008). Nevertheless, even if the water mass tracer property of ε_{Nd} is commonly accepted, our understanding of the complete Nd oceanic cycle is far from being sufficient to allow a reliable use of this proxy as a paleocirculation tracer (Arsouze et al., 2008). In particular, the nature and the relative

[1] By convenience, we preferentially use the ε_{Nd} parameter defined as:

$$\varepsilon_{Nd} = \left(\left({}^{143}Nd/{}^{144}Nd \right)_{sample} \Big/ \left({}^{143}Nd/{}^{144}Nd \right)_{CHUR} - 1 \right) \cdot 10^4,$$

where $\left({}^{143}Nd/{}^{144}Nd \right)_{CHUR} = 0.512638$ is the present averaged earth value (Jacobsen and Wasserburg, 1980).

BGD
6, 5549–5588, 2009

importance of the different sources and sinks, and the dissolved/particulate interactions within the water column are still unconstrained.

Previous studies evidenced a decoupling of the behaviour between Nd concentration and its IC in the open ocean (Bertram and Elderfield, 1993; Jeandel et al., 1995; Tachikawa et al., 1999; Lacan and Jeandel, 2001; Tachikawa et al., 2003). This feature has been named the "Nd paradox" (Tachikawa et al., 2003; Goldstein and Hemming, 2003; Lacan and Jeandel, 2005), and results in different properties characterizing the Nd concentration and its IC distribution in the dissolved phase. Vertical profiles of Nd concentration are similar to that of all Rare Earth Elements, excluding Ce, with low values in surface that increase with depth, suggesting the influence of a vertical cycling (element is scavenged in surface, sinks with the particles, and is subsequently remineralized at depth). Furthermore, Nd concentrations increase along the thermohaline circulation, which is a typical distribution for nutrients like silicate (Elderfield, 1988), whose characteristic residence time is on the order of $\sim 2.10^4$ years (Broecker and Peng, 1982). In contrast, pronounced ε_{Nd} variations between each oceanic basin indicate that the Nd residence time is shorter than the global oceanic mixing time estimated to $\sim 10^3$ years (Broecker and Peng, 1982). A short mixing time is also implied by the "quasi-conservative" property of the tracer, which suggests that ε_{Nd} may vary in the open ocean only by water-mass mixing, excluding vertical cycling.

It was demonstrated that Nd oceanic budgets considering only dissolved river and atmospheric dust inputs failed in balancing both concentration and Nd IC (Bertram and Elderfield, 1993; Tachikawa et al., 2003; van de Flierdt et al., 2004). Other sources have been suggested in order to reconcile the budget of both quantities, like submarine groundwaters (Johannesson and Burdige, 2007) or the "Boundary Exchange" process (BE, strong interactions between continental margin and water masses by co-occurrence of sediment dissolution and Boundary Scavenging (Lacan and Jeandel, 2005). This last process has the advantage to include both a source and a sink to the element, affecting the IC without changing the concentration as observed.

Resolving the "Nd Paradox" hence resides in 1) finding the vertical processes re-

sponsible of both Nd concentration increase with depth and Nd IC conservative property in the water column, and 2) constraining which missing source can explain the important observed Nd IC gradient along the thermohaline circulation together with the relatively small increase of Nd concentration.

Recent modelling of oceanic ε_{Nd}, schematically presented in Fig. 1, helped to improve our understanding of the Nd oceanic cycle. Arsouze et al. (2007, Fig. 1a), taking into account the only BE as a source/sink term, simulated a realistic global ε_{Nd} distribution, suggesting that this process plays a major role in the oceanic cycle of the element. However, this first approach was based on the simulation of the Nd IC only (the Nd concentration being considered constant), using a simple relaxing term parameterization for the BE process. Given that no source flux is explicitly considered in this method, the authors could not address the "Nd paradox" and quantify the processes acting in the oceanic Nd cycle. Jones et al. (2008, Fig. 1b), considering no external sources, but prescribing modelled surface Nd IC with observations, concluded that ε_{Nd} behaves conservatively in the ocean (changing only by water mass mixing), but they needed to invoke an input to the deep North Pacific, which could represent an input directly to the deep ocean (e.g. by boundary exchange), or vertical cycling. However, we underline here that prescribing ε_{Nd} at the surface must be considered as an implicit source of Nd, in contradiction with the conclusion of these authors upon the role of mixing. Lastly, Siddall et al. (2008, Fig. 1c) have modelled explicitly both Nd concentration and IC using a reversible scavenging model for testing the influence of vertical cycling in the oceanic distribution of the element. These authors suggest that both scavenging and remineralisation processes are important for explaining Nd concentration and IC profiles, consistent with Bertram and Elderfield (1993) and Tachikawa et al. (1999, 2003) conclusions. If the results of Siddall et al. (2008) provide important indications to solve the "Nd paradox", the authors could not in return estimates the different fluxes involved in the Nd cycle. Indeed, this study by Siddall et al. (2008) is prescribing Nd concentration and ε_{Nd} to observations in surface waters, and do not explicitly simulate Nd oceanic sources and sinks. This parameterization, although appropriate to initiate

studies using coupled dynamical/biogeochemical models, is insufficient for comprehending the full Nd oceanic cycle and investigating all parts of the "Nd paradox". Also, prescribing Nd IC surface distribution (Jones et al., 2008; Siddall et al., 2008) and Nd concentration, as well as particle distribution (imposed by satellite data and then extrapolated into the water column, Siddall et al., 2008) prevents any paleo-application.

This study proposes to continue the modelling work initiated by Tachikawa et al. (2003), Arsouze et al. (2007) and Siddall et al. (2008) using a coupled dynamical (Ocean Global Circulation Model, that generates dynamical fields)/biogeochemical (dedicated to carbon cycle and ecosystems studies, that simulates particle fields in the ocean) model. The vertical cycling is simulated using a reversible scavenging model developed for the simulation of trace elements with this coupled model (Dutay et al., 2009). Although these authors underlined some limitations of this coupled model for geochemical tracers modelling, as we will see hereafter, our approach is dictated by the wish of collaboration with carbon cycling modellers for further studies that aim at developing the biogeochemical model. That may lead to mutual advance for both carbon cycle and geochemical (Pa, Th, $\delta^{13}C$, Nd, etc.) modelling (Dutay et al., 2009), and also to a significant improvement on our understanding of the element oceanic cycles on long term, mostly in the context of the increasing database that will result from the international GEOTRACES effort (GEOTRACES, 2005). Also, this model is fully prognostic so that it can be easily used for paleo applications or even future climate scenarios.

We explicitly represent and quantify the different sources implied in the oceanic cycle of the element (Fig. 1d). This allows investigating via an independent approach 1) if the BE process could globally represent the primordial flux of the tracer into the ocean, as suggested by Arsouze et al. (2007), and 2) if this process can be associated to the "missing flux" proposed by Tachikawa et al. (2003) in order to balance Nd oceanic budget.

Besides being a potential capital component for Nd oceanic cycle, the determination of trace element sources is essential to better constrain the general lithogenic flux

to the ocean. It is important to understand the effects of erosion fluxes on ocean chemistry, and more particularly on primary production and sedimentation. Studying the BE process may provide substantial information on general geochemical cycle of the elements, such as carbon and iron, which have a direct impact on climate change.

2 Modelling the Nd oceanic cycle

2.1 The dynamical model NEMO-OPA

The dynamical model used is the NEMO-OPA model (IPSL/LOCEAN, Madec, 2008). It includes the sea-ice model LIM (Louvain-La Neuve, Fichefet and Maqueda, 1997), in its low-resolution configuration ORCA2. The definition of the mesh is based on a $2^{\circ}\times2^{\circ}\times\cos$ (latitude) MERCATOR grid, with poles defined on the continents so as to get rid of singularities near the North Pole. Meridional resolution increases to 0.5° near the equator, in order to take into account the specificities of local dynamics. Vertical resolution varies with depth, from 10 m at surface (12 levels included in the first 125 m) to 500 m at the bottom (31 levels on total). The model is forced at the surface by heat and freshwater fluxes obtained from bulk formulae and ERS satellite data on the tropics, and NCEP/NCAR data on polar regions. Surface salinity is readjusted every 40 days to monthly WA01 data to prevent from a drift of the model (Timmermann et al., 2005). The Turbulent Kinetic Energy closure is applied in the mixing layer (Blanke and Delecluse, 1993), and subscale physics is parameterized using the Gent and McWilliams scheme (1990). The same model, in similar configurations, has already been used for other geochemical tracer simulations (Dutay et al., 2002, 2004; Doney et al., 2004; Arsouze et al., 2007). Despite classical shortcomings of low resolution models (boundary currents too weak, crude representation of sinking of dense water during deep water masses formation), it satisfyingly simulates the main structures of the global thermohaline circulation.

2.2 The biogeochemical model PISCES

The biogeochemical model PISCES developed for carbon cycle modelling was coupled to NEMO. It is a prognostical ecosystem and oceanic carbon cycle model, based on the Hamburg Model of Carbon Cycle version 5 (HAMOCC5, Aumont et al., 2003), that represents the biogeochemical cycles of carbon, oxygen, and five nutrients of primary production (phosphates, nitrates, silicates, ammonium and iron). Redfield ratios are set to be constant, and are based on a phytoplankton growth limited by nutrients availability (Monod, 1942).

The model features two classes of phytoplankton (nanophytoplankton and diatoms), and two classes of zooplankton (microzooplankton and mesozooplankton), as well as three non-living compartments, including Dissolved Organic Carbon (DOC), small and large particles. Small particles (particles with a size between 2 and 100 μm) have a sinking velocity of 3 m/day (determined using relationship between the size of the particle and the sinking velocity established by Kriest, 2002), and consist of Particulate Organic Carbon (POCs). The large particles pool includes Particulate Organic Carbon with a diameter larger than 100 μm (POCb), biogenic silica (BSi), calcite ($CaCO_3$) and lithogenic particles (atmospheric dust), sinking with a velocity varying from 50 m/day at surface to 300 m/day at depth. The two classes of POC interact via the processes of aggregation/disaggregation. Also remineralization process between POCs and DOC is represented. The reference of 100 μm used to differentiate small and large carbonate particles (POCs and POCb) does not correspond to the definition used by experimentalists, who usually refer to large particles as the particles collected in traps or by large volume filtration and with a diameter larger than 50 μm. This being so, the size range of particles trapped remains unknown. In addition, the particles observed by the Underwater Video Profilers (UVP, Gorsky, 2000) have a diameter larger than 100 μm meaning the same limit as prescribed in the model.

A more detailed description of the model, as well as the equations used, are available as supplementary material of Aumont and Bopp (2006).

An evaluation of the particle fields generated by the PISCES model with available data collected by particles traps, satellite observations and estimations was performed by Gehlen et al. (2006) and Dutay et al. (2009). The small particle pool represents the main particle stock in surface (at least one order of magnitude higher than the large particle concentration). The simulated small particle concentrations in surface waters are in agreement with the observations, mostly in the regions of high productivity (coastal upwellings, Equatorial Pacific, Austral Ocean). Contrastingly, PISCES generates exaggerated vertical variations of the small particle distributions in the water column leading to too low concentrations in small particles at depth, due to remineralization and aggregation processes. This POCs vertical gradient largely overestimates the available observations (only a factor 50 between surface and depth, compared to a factor 1000 for the model). On the opposite, the model succeeds to generate the few $CaCO_3$ and BSi vertical profiles observed in the water column (Dutay et al., 2009).

2.3 The reversible scavenging model

The increase of the Nd concentration with depth suggests a reversible exchange between the dissolved and the particulate phases (Nozaki and Alibo, 2003). Nd gets adsorbed onto sinking particles in the surface layers, and is redissolved at depth (we refer to all these processes by vertical cycling). In order to represent this process, we used the approach developed by Nozaki et al. (1981) and Bacon and Anderson (1982), and reformulated by Henderson et al. (1999), Siddall et al. (2005) and Dutay et al. (2009) for ^{231}Pa and ^{230}Th modelling. It considers that dissolved and particulate phases are in equilibrium within the ocean, and their relative contribution is set using an equilibrium partition coefficient K.

Considering Nd dissolved concentrations (Nd_d) and Nd particulate concentrations (concentration of Nd by unity of particle mass, Nd_p), the equilibrium partition coefficient

K is defined as:

$$K = \frac{\mathrm{Nd}_p}{\mathrm{Nd}_d C_p} \quad (1)$$

where C_p is the mass of particles normalized to the fluid density. This coefficient K is defined for each type of particles represented in the model: small (POCs) and big (POCb) Particulate Organic Carbon, Biogenic Silica (BSi), calcite ($CaCO_3$) and lithogenic atmospheric dust (litho).

The two isotopes ^{143}Nd and ^{144}Nd were modelled independently and $\varepsilon_{\mathrm{Nd}}$ and Nd concentration were calculated afterward. Observations do not suggest any fractionation between ^{143}Nd and ^{144}Nd dissolved, colloidal and particulate phases (Dahlqvist, 2005), as they are two isotopes of a same element, and their masses are quite similar. Partition coefficients (K) are thus taken identical for the two isotopes for each particle type.

In the model, we transport total Nd concentration for each tracer ($^{143}\mathrm{Nd}_T$ and $^{144}\mathrm{Nd}_T$), defined as the sum of dissolved concentration, small (POCs: Nd_{ps}) and big (POCb, BSi, $CaCO_3$, litho : Nd_{pb}) particulate concentration. We obtain:

$$\mathrm{Nd}_T = \mathrm{Nd}_{ps} + \mathrm{Nd}_{pb} + \mathrm{Nd}_d = (K_{\mathrm{POCs}} \times C_{\mathrm{POCs}} + K_{\mathrm{POCb}} \times C_{\mathrm{POCb}} + K_{\mathrm{BSi}} \times C_{\mathrm{BSi}} + K_{\mathrm{CaCO_3}} \times C_{\mathrm{CaCO_3}} + K_{\mathrm{litho}} \times C_{\mathrm{litho}} + 1) \times \mathrm{Nd}_d \quad (2)$$

that leads to:

$$\mathrm{Nd}_{ps} = \frac{K_{\mathrm{POCs}} \times C_{\mathrm{POCs}}}{K_{\mathrm{POCs}} \times C_{\mathrm{POCs}} + K_{\mathrm{POCb}} \times C_{\mathrm{POCb}} + K_{\mathrm{BSi}} \times C_{\mathrm{BSi}} + K_{\mathrm{CaCO_3}} \times C_{\mathrm{CaCO_3}} + K_{\mathrm{litho}} \times C_{\mathrm{litho}} + 1} \times \mathrm{Nd}_T \quad (3)$$

$$\mathrm{Nd}_{pb} = \frac{K_{\mathrm{POCb}} \times C_{\mathrm{POCb}} + K_{\mathrm{BSi}} \times C_{\mathrm{BSi}} + K_{\mathrm{CaCO_3}} \times C_{\mathrm{CaCO_3}} + K_{\mathrm{litho}} \times C_{\mathrm{litho}}}{K_{\mathrm{POCs}} \times C_{\mathrm{POCs}} + K_{\mathrm{POCb}} \times C_{\mathrm{POCb}} + K_{\mathrm{BSi}} \times C_{\mathrm{BSi}} + K_{\mathrm{CaCO_3}} \times C_{\mathrm{CaCO_3}} + K_{\mathrm{litho}} \times C_{\mathrm{litho}} + 1} \times \mathrm{Nd}_T \quad (4)$$

This allows defining Nd concentrations in small and big particles a posteriori as a function of partition coefficients and total Nd concentration. The main advantage of this method is that we simulate explicitly the total concentration of the two isotopes (two tracers $^{143}Nd_T$ and $^{144}Nd_T$) rather than concentration in every phase (dissolved, small particles and all big particles, meaning 12 tracers), which implies a substantial gain of computational cost.

The evolution of the total concentration of the tracer is equal to the sum of all sources (A), influence of vertical cycling (B) and physical transport by advection and diffusion (C). The conservation equation of the tracer can therefore be written:

$$\frac{\partial Nd_T}{\partial t} = \underbrace{S\,(Nd_T)}_{(A)} \underbrace{-\frac{\partial (w_s Nd_{ps})}{\partial z} - \frac{\partial (w_b Nd_{pb})}{\partial z}}_{(B)} \underbrace{-U \cdot \nabla Nd_T + \nabla \cdot (k \nabla Nd_T)}_{(C)} \quad (5)$$

where $S(Nd_T)$ is the Source term of the tracer (cf. Sect. 2.4). The vertical cycling represents the scavenging of Nd by the particles (w_s and w_b are the sinking velocities of small and big particles, respectively). The simulations are performed "off-line" using pre-calculated dynamical: velocity (U) and mixing coefficient (k), and particle (POC_s, POC_b, BSi, and $CaCO_3$) distributions in order to reduce computational costs, which allows us to perform some sensitivity tests.

2.4 Description of Nd sources

One of our objectives was to study the relative influence of the different sources of Nd to the ocean. We therefore explicitly represent the different source of Nd in the ocean in our simulations.

The source of the BE process is supposed to be the dissolution of a small percentage of the sediments deposited along the continental margin. We specify this source in the model by imposing an input flux on each continental margin grid point of the model between 0 and 3000 m (Boillot and Coulon, 1998). This Nd continental source is written

as:

$$S(A_T)_{sed} = \int_V F_{sed} * mask_{mar} * f(z) \quad (6)$$

where F_{sed} is the source flux of sedimentary Nd to the ocean (in g(Nd)/m^3/yr), assumed here as geographically constant. This hypothesis may be not verified in the ocean and disparities could play an important role on global scale. However, considering the actual poor knowledge of the processes acting in this source, it seems reasonable to set it constant as a first approximation. This flux is multiplied by the percentage of surface of continental margin in each grid cell of the model ($mask_{mar}$), determined using the high resolution ETOPO-2 bathymetry, as well as by a vertical function equal to 1 in the first 1000 m, then exponentially decreasing at depth ($f(z)$). This vertical variation has been applied in accordance with iron modelling (Aumont and Bopp, 2006) and previous ε_{Nd} modelling studies (Arsouze et al., 2007), because we suppose that the sediment dissolution is more important in surface than at depth (dynamical activity more vigorous, biological processes more important). The only available global estimation of the Nd continental margin flux is the "missing flux" calculated by Tachikawa et al. (2003). We have then used their value of 8.0×10^9 g(Nd)/yr as a reference for our simulations. ^{143}Nd and ^{144}Nd isotope concentrations are determined using Nd concentration and ε_{Nd} maps along the continental margins, generated by interpolation of a recent data compilation (Jeandel et al., 2007, and Fig. 2a and b).

Nd inputs in surface waters (first vertical level) taken into account in our simulations are dissolved river discharge (defined on continental margin points only) and atmospheric dust deposit.

$$S(A_T)_{surf} = \int_V F_{surf} \quad (7)$$

where F_{surf} is the Nd flux of these two sources to the ocean (in g(Nd)/m^3/yr).

For dissolved river discharge we used the climatological runoff applied to the dynamical model (Fig. 2c). Nd IC (Fig. 2d) and concentrations (Fig. 2e) in rivers inputs are

estimated using the compilation of data provided by Goldstein and Jacobsen (1987). Using the runoff estimation provided by the NEMO model, and a subtraction of 70% of material in the estuaries (Sholkovitz, 1993; Elderfield et al., 1990; Nozaki and Zhang, 1995), we obtain Nd dissolved flux from rivers of 2.6×10^8 g(Nd)/yr (Table 1). This value is lower than the flux used by Tachikawa et al. (2003), equal to 5×10^8 g(Nd)/yr.

Atmospheric dust flux is determined using monthly maps provided by Tegen and Fung (1995), in agreement with what was done in PISCES model for nutrients (Aumont and Bopp, 2006). Nd IC of this source has been established using available data (Grousset et al., 1988, 1998). However, when no data were available, we applied the ε_{Nd} value of the source region of the dusts (Fig. 2f). Nd concentration in atmospheric dusts was set to be constant to 20 μg/g (Goldstein et al., 1984). We considered a 2% Nd dissolution rate (Greaves et al., 1994), as used by Tachikawa et al. (2003). It is important to note that some uncertainty remains concerning dissolution rate of atmospheric dusts, as published data vary from 2 to 50% (Tachikawa et al., 1999; Greaves et al., 1994). However, Zhang et al. (2008) reconsidered all these data and finally estimate that this percentage does not exceed 10%. We finally obtain a flux of 1×10^8 g(Nd)/yr (Table 1). Still, this value is lower than Tachikawa et al. (2003) who considered earlier Duce et al. (1991) atmospheric dusts deposit estimation, leading to a flux of 5×10^8 g(Nd)/yr. Sensitivity tests on both dissolution rate ratio for atmospheric dusts and Nd dissolved river discharge (not shown here) do not significantly change the results and conclusions presented here.

The re-dissolution of solid material deposited by rivers at the estuary mouths is potentially a source of great importance (Sholkovitz, 1993; von Blanckenburg et al., 1996). However, this source is implicitly taken into account via the BE source (F_{sed}), as we consider that all material deposited along the continental margin is made available for sediment re dissolution.

To balance the budget of Nd in the ocean, the only Nd sink considered is the burying of particles in the sediment at the deepest level of the model. Simulations are run until ^{143}Nd and ^{144}Nd oceanic concentrations reach an equilibrium state, which is when the

sink balances global sources.

3 Simulation description

So far, the available observations of Nd concentrations in particulate phases allowing constraining the values of the equilibrium partition coefficients (K) are very scarce. In addition, the pool of particles generated by the PISCES model is biogenic, whereas data suggest that particulate Nd, is mainly adsorbed on the hydroxydes phases coating the biogenic particles (Sholkovitz et al., 1994). Nd concentrations in iron or manganese hydroxydes are at least an order of magnitude higher than those observed for biogenic particles (Bayon et al., 2004). The fact that PISCES does not take into account these particles might be critical to simulate realistic Nd dissolved-particulate interactions. Nevertheless, observations in the Atlantic and Austral basins, give an estimation of A_p/A_d value between 0.05 and 0.1 (Jeandel et al., 1995; Tachikawa et al., 1997; Zhang et al., 2008).

Using the same model for their ^{231}Pa and ^{230}Th simulations, Dutay et al. (2009) have shown the necessity to impose a variation of the partition coefficient as a function of particle stock, in order to simulate realistic vertical profiles for both the dissolved and particulate phases. In addition, the scavenging of these tracers had to be controlled by the small particle pool, and thus the value of their partition coefficients with this pool had to be superior to those applied to the big particles. We have taken up this expertise for our Nd simulation and therefore set equilibrium partition coefficients for the big particle pools lower than those for the small particle pool.

Lastly, we assumed that there is no preferential scavenging of Nd when biogenic silica or carbonate dominate the particle pool. We then only differentiate small and big particles. Same value of equilibrium partition coefficient value is taken for each pool of big particles, considering their global averaged concentrations (POCb, BSi, $CaCO_3$ et litho). Characteristics of sensitivity tests performed are summarized in Table 1.

The first experiment (EXP1) takes into account only dissolved river discharge and

atmospheric dust (surface sources), which are the classical sources generally considered in trace element budget studies. In addition only small and lithogenic particles are taken into account to simulate the vertical cycle, leaving the study of the influence of biogenic large particles for further sensitivity tests. We take $K_{POMs}=1.4\times10^{7}$ and $K_{litho}=2.3\times10^{6}$ that corresponds to $A_P/A_d=0.001$ and 1×10^{-4} respectively, and K=0 for remaining particle pools (POMb, $CaCO_3$, bSi, cf. Table 1). These values are much lower than the available data, but about the same order of magnitude as in Siddall et al. (2008).

In a second experiment (EXP2), we consider the same configuration as the first simulation, but we added the sediment remobilization (source of the BE process).

EXP3 and EXP4 correspond to sensitivity tests of the vertical cycling, considering the same sources of Nd as those considered in EXP2. For the third experiment (EXP3), we enhanced the small particle role relative to EXP2 by increasing the value of the equilibrium partition coefficient on small particles to $K_{POMs}=7.7\times10^{7}$ (which is equivalent to $A_P/A_d=0.005$). In the fourth experiment (EXP4) we have inserted the big particles (POMb, $CaCO_3$, BSi) that were neglected in the three first experiments, the other equilibrium partition coefficients being identical to those of EXP2. The equilibrium partition coefficient value for big particles in EXP4 is set two orders of magnitude lower than for small particles, considering their respective concentrations in the PISCES model, i.e. $K_{POCb}=2.6\times10^{4}$, $K_{BSi}=1.8\times10^{4}$ and $K_{CaCO_3}=7.8\times10^{4}$ that correspond to $A_p/A_d=1\times10^{-4}$ (Table 1).

Finally, in the last experiment (EXP5) we optimized the characteristics of both our dynamical and biogeochemical models according to the information gained through the previous sensitivity tests, in order to produce the most realistic simulation. BE flux is adjusted to $F(A_T)_{sed}=1.1\times10^{10}$ g(Nd)/yr and equilibrium partition coefficients are slightly reduced compared to EXP4 for POMb, $CaCO_3$, BSi and litho, and unchanged for the small particles (Table 1). Depending on the estimations, only between 3 and 5% (Milliman and Syvitski, 1992) dissolution of Nd material is required to explain our total BE flux $S(A_T)_{sd}=1.1\times10^{10}$ g(Nd)/yr.

4 Results

For each experiment, both Nd IC and concentration are shown along meridional sections in the Pacific Ocean (averaged zonally between 120° W and 160° W) and along the western boundary of the Atlantic Ocean (Figs. 3 and 5), where the water mass ε_{Nd} have been characterized. Figures 4 and 6 show scatter plot of model and observations and Figs. 7 and 8 display horizontal maps of ε_{Nd} in surface (0–200 m) and at depth (800–5000 m), respectively.

First experiment (EXP1) produces a satisfying ε_{Nd} distribution in surface waters (Fig. 7), but much too homogeneous in the deep ocean (Figs. 3, 5 and 8), particularly in the Atlantic basin, where the signature of the main water masses (NADW, AAIW, AABW) are not correctly simulated. Moreover, the Nd concentrations are at least an order of magnitude too low compared to the observations (2.3 pmol(Nd)/kg, $[Nd]_{obs}$=21.5 pmol(Nd)/kg).

In the second experiment (EXP2, BE added), simulated ε_{Nd} values in surface waters are still in agreement with the data, and its distribution in the deep Atlantic Ocean is closer to the data. Indeed, this basin water masses are now simulated with very realistic ε_{Nd} values (Fig. 3): AABW ($\varepsilon_{Nd\,model} \cong -10$, $\varepsilon_{Nd\,obs} \sim 8$) but also AAIW ($\varepsilon_{Nd\,model} \cong -8$, $\varepsilon_{Nd\,obs} \sim 8$) and NADW ($\varepsilon_{Nd\,model} \cong -13$, $\varepsilon_{Nd\,obs} \sim 13$). Contrastingly, simulated ε_{Nd} values in the deep Pacific Ocean are still much too negative when compared with the observations ($\varepsilon_{Nd\,model} \cong -10$, $\varepsilon_{Nd\,obs} = -4$, Fig. 8), hence producing a much too homogeneous ε_{Nd} inter-basin gradient. The simulated Nd concentrations (Figs. 5 et 6) display now too high values in the global ocean ($[Nd]_{model}$=35.7 pmol(Nd)/kg). The Nd vertical profiles are too pronounced, with realistic values at intermediate depth in both the Atlantic and Pacific basins, but concentrations are too low in surface waters, and too high at depth, particularly in the Pacific basin (Figs. 5 and 6). It should also be noted that this simulation produces a realistic increase of concentrations along the thermohaline circulation, in agreement with the observations.

Increasing the value of equilibrium partition coefficient on small particles in the third

experiment (EXP3) leads to a strengthening of the vertical cycling effect on simulated ε_{Nd} and Nd concentrations. It results in an undesirable vanishing of NADW isotopic signature along its pathway in the Atlantic Ocean (Fig. 3). However it improves the ε_{Nd} distribution in the deep Pacific Ocean where values gets more radiogenic (Fig. 8), but also leads to unrealistic high values at intermediate depths. Increasing vertical cycling enhances the sedimentation process (sink of Nd), and reduces the oceanic residence time of the tracer from ~700 years in EXP 1 and 2 to 150 years in EXP3 (Table 1). It then excessively reduces the simulated Nd concentrations ($[Nd]_{model}$=6.8 pmol(Nd)/kg).

Taking into account the influence of fast sinking biogenic big particles (POMb, $CaCO_3$, bSi; EXP4) yields results close to those observed when increasing the equilibrium partition coefficient for small particles (EXP3): the oceanic residence time of the tracer decreases (125 years), and both Nd concentration and Nd IC in the water column are more homogeneous . Simulated Nd IC distribution in the deep Pacific Ocean is in better agreement with the observations than in EXP2, but Nd concentration becomes too low. Most of all, this simulation succeeds in keeping a realistic isotopic signature of the main water masses in the Atlantic basin, and especially for NADW (Fig. 3).

Finally in the last experiment (EXP5) in which intensity of the BE flux and values of partition coefficients of large particles have been adjusted, we simulate ε_{Nd} distribution in excellent agreement with the data (71% fit in the ε_{Nd} (model)=ε_{Nd} (data) ±3 ε_{Nd} envelop, Figs. 3 and 4). In particular, inter-basin ε_{Nd} gradients (Fig. 8) and isotopic signature of the main water masses (Fig. 3) are correctly reproduced, as well as surface and intermediate isotopic signatures (Fig. 7). As observed in EXP4, the scavenging onto big particles leads to more coherent vertical gradients, particularly for the concentration (Fig. 5). The increase of the Nd sink has been compensated by an increase of the sediment remobilization process to produce more coherent concentrations (Fig. 6, average global value of $[Nd]_{model}$=24.6 pmol(Nd)/kg) and a more realistic residence time of 360 years, when compared to other estimations.

BGD
6, 5549–5588, 2009

5 Discussion

5.1 Sensibility of Nd oceanic cycle to sources

The above results provide valuable information about the role (or impact) of the different Nd sources on the oceanic Nd IC and concentration distributions. This information allows a better understanding of one of the aspect of the Nd paradox: how can we explain the important observed Nd IC gradient along the global thermohaline circulation despite a relatively small increase of Nd concentration?

In our first experiment, we first applied dissolved river discharge and atmospheric dust (F_{surf} – EXP1). This lead to simulated ε_{Nd} that are close to the existing data at surface depth (0–200 m, Fig. 7), suggesting that these sources could control the isotopic Nd distribution in the upper ocean. However, it produces an ε_{Nd} distribution that is too homogeneous in the deep ocean, too negative values in the deep Pacific, and a very poor simulation of water masses signature in the Atlantic Ocean. A possible way to improve the results in the Pacific Ocean would be to enhance vertical cycling (either by increasing the equilibrium partition coefficient for the small particles or by inserting the big particles in the scavenging model), in order to bring the radiogenic signature of surface water to depth. However, this action yielded an increase of Nd sedimentation and subsequently a decrease of the global Nd concentration. Since the simulated Nd concentrations in EXP1 are already an order of magnitude lower than the observed concentrations, increasing the vertical cycling does not help to reconcile both Nd IC and concentration distributions, as much as the sources are restricted to the surface ones only.

Another option for improving the simulated deep Pacific and Atlantic ε_{Nd} distributions was to consider an additional source of Nd to the oceanic reservoir. Sediment re-dissolution effect along the continental margin has been tested in the second experiment (EXP2). Its flux ($S(A_T)_{sed}$) intensity was estimated using first the "missing flux" proposed by Tachikawa et al. (2003) and then adjusted in EXP5. Taking into account this source largely improved our simulation of the Nd oceanic cycle, generating Nd con-

centrations closer to the data, though still an order of magnitude lower. It also improved drastically the simulation of the isotopic composition of the main water masses in the Atlantic Ocean.

The Nd oceanic budget simulated here suggests a large predominance (about twenty times higher than cumulated other sources) of the role of the sediment re-dissolution source ($S(A_T)_{sed}$), meanwhile surface sources ($S(A_T)_{surf}$) appeared predominant for constraining surface waters isotopic signature. Other experiments, not reported here, showed that considering BE only, excluding dissolved river and dust inputs, lead to less realistic simulations of the surface ε_{Nd} distributions. As a source that sets Nd concentration and Nd IC at depth, we can preclude submarine groundwater as acting in BE, as their influence is mainly limited to the 200 upper meters.

Changing the solubility of atmospheric dust entering seawater or reducing the subtraction of dissolved material in the estuaries (which would contradict the field or experimental results) may change the $S(A_T)_{surf}$ value. However, this latter value still remains small compared to $S(A_T)_{sed}$ value, and the change finally does not significantly modify the Nd distribution (sensitivity tests not presented here). Boundary Exchange can therefore be considered as a major source of Nd in the ocean that is fundamental to simulate a realistic Nd oceanic cycle.

5.2 Sensitivity of Nd oceanic cycle to vertical cycling: small vs. big particles

The second experiment succeeded to simulate reasonable distribution of both Nd IC and concentrations. However, some discrepancies still remain, particularly in the deep Pacific where simulated deep waters had underestimated Nd IC and overestimated concentrations. Enhancing vertical cycling in order to homogenize the vertical column in the Pacific is therefore pertinent, though it should maintain the performance in the Atlantic Ocean. Indeed, the lateral isopycnal transport being more important in the Atlantic than in the Pacific, vertical processes in this last basin might be more sensitive.

Basically, the equilibrium partition coefficient establishes the relative influence between dynamical lateral transport and vertical scavenging. Enhancing the influence of

vertical cycling, either by increasing the partition coefficient for small particles (EXP3), or by inserting big particles in the reversible scavenging model (EXP4), increased the removal of Nd from the water column, and reduces our global Nd concentration to more unrealistic values (cf. Table 1, Figs. 5 and 6).

Both EXP3 and EXP4 succeeded to generate the requested reduction of Nd concentration, and the formation of more radiogenic waters in the deep Pacific Ocean (Figs. 3, 4 and 8). However they differed in their performance in the Atlantic Ocean. EXP3 generated a significant degradation of simulated ε_{Nd} characteristics in the Atlantic Ocean, while EXP4 preserved and even improved the remarkable agreement with the data, in the Atlantic basin.

These results are consistent with those of Siddall et al. (2008), which demonstrated the importance of vertical cycling (reversible scavenging process) in reconciling Nd IC and concentration distributions, and therefore resolving the "Nd paradox". The model presented here underlines the influence of different pools of particles size for setting the characteristics of the Nd isotopic distribution, and more precisely the potential role of fast sinking particles.

5.3 Resolving the "Nd paradox"

The configuration of our last experiment (EXP5) was elaborated considering the expertise gained from sensitivity tests on sources and vertical cycling, our target being to get the best agreement between simulations and data. We have considered the surface sources of EXP1 ($S(A_T)_{surf}$=2.6×10^8 g(Nd)/yr) whereas the sediment remobilization has been slightly increased ($S(A_T)_{sed}$=1.1×10^{10} g(Nd)/yr), in order to compensate the decrease in Nd concentration caused by the insertion big particles in the reversible scavenging model. Associated with this later source, the sink of Nd along the continental margin (corresponding to the Boundary Scavenging process) represents 64% of the global Nd sink (Fig. 9), confirming that BE acts as both a major source and sink term for Nd.

Due to the limited number of sensitivity experiments that could be conducted due to

time constraints, this version is not necessarily optimal, but it shows some significant improvements compared to the fourth other experiments. The resulting simulated Nd IC is in excellent agreement with the data (Figs. 3 and 4), though concentrations persist to be rather too elevated in the deep ocean (Figs. 5 and 6). We attribute this bias to the particulate fields generated by the biogeochemical model PISCES. In this work, as in the ^{231}Pa and ^{230}Th simulations proposed by Dutay et al. (2009), and consistent with either experimental or field observations, the small particles pool drives the vertical cycling in the water column. It is characterized here with a higher equilibrium partition coefficient for small particles than for the big particles pool. However, small particle fields generated by PISCES are underestimated at depth (Dutay et al., 2009) leading to an overestimation of the Nd concentrations (as Nd is less scavenged). Improving the small particle concentration at depth in the PISCES model would likely help to recover deep Pacific radiogenic waters in our simulation (Figs. 3 and 8), better simulate element cycles in the ocean, which is an important goal. Nevertheless, our model demonstrated that big particles also play an important role, in reconciling deep ocean Nd concentration while keeping Nd IC water-mass tracer property.

The residence time of Nd in the ocean in this last experiment is 360 years, which is in the lower range of previous estimations of ~300 to ~600 years (Piepgras and Wasserburg, 1983; Jeandel et al., 1995; Tachikawa et al., 1999, 2003; Siddall et al., 2008). This value is still consistent with the heterogeneity of the Nd distribution between the different oceanic basins. All together, these factors suggest that BE is a major primordial source for Nd oceanic cycle, and that in conjunction with vertical cycling (reversible scavenging), it provides the means to reconcile the "Nd paradox". The first estimation of the order of magnitude of the "missing flux" proposed by Tachikawa et al. (2003) is confirmed by our model results. The reversible scavenging is also essential to explain the Nd nutrient-like profile in the water column and the water mass tracer property of Nd IC, in agreement with recent REE modelling studies (Nozali and Alibo, 2003; Siddall et al., 2008; Oka et al., 2008).

However, if BE is evidenced as the source term that allows explaining the large Nd

IC variation observed along the global thermohaline circulation, without large Nd concentration change (due to the associated Boundary Scavenging sink, Fig. 9), still remains the question raised by apparent contradiction of conservativity of Nd IC and non conservativity of Nd concentration. This critical point has to be addressed in another dedicated study, so as to fully resolve the "Nd paradox".

6 Conclusions

The objective of this study was to use an ocean model as a tool to better understand the Nd oceanic cycle and to work toward the resolution of the "Nd paradox", (i.e. estimating the sources and sink of the element, and qualifying the processes acting on the element's distribution within the reservoir). We simultaneously simulated both Nd IC and concentration using a fully prognostic coupled dynamical/biogeochemical model and used a reversible scavenging model to simulate the Nd transformation and sink into the ocean. We have also implemented for the first time a realistic calculation of the Nd sources, with an explicit representation of sedimentary remobilization along continental margin (source of the BE process) as well as dissolved river discharge and atmospheric dust sources (surface sources).

In accordance with previous results of Siddall et al. (2008) and Oka et al. (2008), we need to invoke vertical cycling (surface substraction combined with remineralisation at depth) to correctly simulate Nd IC and concentration distributions. We are as yet unable to verify the validity of our partition coefficients because very little data are available so far. A strong recommendation deduced from this work is to improve our knowledge of the dissolved/particle distribution of the geochemical tracers, which the GEOTRACES program should make possible. Our performance in simulating Nd concentration is also still limited by our models. Especially, the too low concentration in small particles field simulated at depth by PISCES model is very likely the cause for overestimated Nd concentrations in the deep Pacific Ocean. This work also suggests that it is important to consider different kinds of particles, and especially their sinking velocity, in setting

the characteristics of the Nd isotopic distribution. This study can therefore be used as a basis for improving the representation of the complexity of observed particle field distribution in the models, such as considering a whole continuous spectrum of particle size (Gehlen et al., 2006).

The simulations performed strongly suggest that sediment remobilization is the main Nd source to the oceanic reservoir, with a flux of 1.1×10^{10} g(Nd)/yr. In addition to it acting as a source, the Boundary Scavenging also represents up to 64% of the total Nd sink. We suggest that Boundary Exchange is likely the "missing source term" mentioned by Tachikawa et al. (2003) that could reconcile both Nd IC and concentration oceanic budgets. The fact that this potential source has not been considered so far, despite large amount of Nd available from solid material from river discharge deposited on the continental margin, may resides on the very small amount of dissolution (3–5%) required to obtain these fluxes. Nd isotopes thus appear as a powerful tool to quantify this margin source to this ocean, that may not only involve Nd, but may have a more general significance for the ocean chemistry. Dissolved river discharge (2.6×10^{8} g(Nd)/yr), and atmospheric dusts (1.0×10^{8} g(Nd)/yr) play only a significant role on surface ε_{Nd} distribution. The residence time of Nd in the ocean, calculated in this configuration, is estimated to be 360 years, which is in agreement with previous estimates.

The high computational cost for one simulation was a limiting factor for sensitivity tests on sources and equilibrium partition coefficients. Optimal values on parameters of the model may not be those used for experiment EXP5, but we are confident that our main results are robust. One easily envisaged improvement could be the use of the Transport Matrix Method (Khatiwala et al., 2005) for this model, to better optimize these parameters.

However, if this study highlights the predominant role of BE on Nd oceanic cycle, we have no indication of chemical, biological or physical processes that act on this sediment re-dissolution. It then appears to be quite important for the geochemical community to pay attention on continental margins/open ocean interfaces to determine if the

"Boundary Scavenging" (observed for Be and Pa/Th, Anderson et al., 1990) is compensated by lithogenic inputs for other chemical tracers, and how this input is materialized: cold hydrothermalism on margins, remobilization and dissolution of sediments after resuspension, early diagenesis or both, water penetration in sediments, etc.

This implies a multi-tracers approach, in particular with highly reactive elements such as ^{231}Pa and ^{230}Th. Also, it seems inevitable to improve and adapt biogeochemical models to the simulation of trace elements, such integrating iron manganese or oxyde crusts that are supposed to be main carriers of these tracers.

The publication of this article is financed by CNRS-INSU.

References

Anderson, R. F., Lao, Y., Broecker, W. S., Trumbore, S. E., Hofmann, H. J., and Wolfli, W.: Boundary scavenging in the Pacific Ocean: a comparison of ^{10}Be and ^{231}Pa, Earth Planet. Sc. Lett., 96, 287–304, 1990.

Arsouze, T., Dutay, J. C., Lacan, F., and Jeandel, C.: Modeling the neodymium isotopic composition with a global ocean circulation model, Chem. Geol., 239, 165–177, 2007.

Arsouze, T., Dutay, J.-C., Kageyama, M., Lacan, F., Alkama, R., Marti, O., and Jeandel, C.: A modeling sensitivity study of the influence of the Atlantic meridional overturning circulation on neodymium isotopic composition at the Last Glacial Maximum, Clim. Past, 4, 191–203, 2008, http://www.clim-past.net/4/191/2008/.

Aumont, O., Maier-Reimer, E., Blain, S., and Monfray, P.: An ecosystem model of the

global ocean including Fe, Si, P colimitations, Global Biogeochem. Cy., 17, 2, 1060, doi:10.1029/2001GB001745, 2003.
Aumont, O. and Bopp, L.: Globalizing results from ocean in situ iron fertilization studies, Global Biogeochem. Cy., 20, 2, GB2017, doi:10.1029/2005GB002591, 2006.
Bacon, M. P. and Anderson, R. F.: Distribution of thorium isotopes between dissolved and particulate forms in the Deep-Sea., J. Geophys. Res., 87, 2045–2056, 1982.
Bayon, G., German, C. R., Burton, K. W., Nesbitt, R. W., and Rogers, N.: Sedimentary Fe-Mn oxyhydroxides as paleoceanographic archives and the role of aeolian flux in regulating oceanic dissolved REE, Earth Planet Sc. Lett., 224, 477–492, 2004.
Bertram, C. J. and Elderfield, H.: The geochemical balance of the rare earth elements and Nd isotopes in the oceans, Geochim. Cosmochim. Ac., 57, 1957–1986, 1993.
Blanke, B. and Delecluse, P.: Variability Of The Tropical Atlantic-Ocean Simulated By A General-Circulation Model With 2 Different Mixed-Layer Physics, J. Phys. Oceanogr., 23, 1363–1388, 1993.
Boillot, G. and Coulon, C.: La déchirure continentale et l'ouverture océanique – Géologie des marges passives., Overseas Publishers Association, Gordon and Breach Science Publishers, 1998.
Broecker, W. S. and Peng, T. H.: Tracers in the Sea, Eldigio Press, Palisades, N.Y., 690 pp., 1982.
Dahlqvist, R., Andersson, P. S., and Ingri, J.: The concentration and isotopic composition of diffusible Nd in fresh and marine waters, Earth Planet. Sc. Lett., 233, 9–16, 2005.
Doney, S. C., Lindsay, K., Caldeira, K., Campin, J. M., Drange, H., Dutay, J. C., Follows, M., Gao, Y., Gnanadesikan, A., Gruber, N., Ishida, A., Joos, F., Madec, G., Maier-Reimer, E., Marshall, J. C., Matear, R. J., Monfray, P., Mouchet, A., Najjar, R., Orr, J. C., Plattner, G. K., Sarmiento, J., Schlitzer, R., Slater, R., Totterdell, I. J., Weirig, M. F., Yamanaka, Y., and Yool, A.: Evaluating global ocean carbon models: The importance of realistic physics, Global Biogeochem. Cy., 18, 3, GB3017, doi:10.1029/2003GB002150, 2004.
Duce, R. A., Liss, P. S., Merrill, J. T., Atlas, E. L., Buat-Ménard, P., Hicks, B. B., Miller, J. M., Prospero, J. M., Arimoto, R., Church, T. M., Ellis, W., Galloway, J. N., Hansen, L., Jickells, T. D., Knap, A. H., Reinhardt, K. H., Schneider, B., Soudine, A., Tokos, J. J., Tsunogai, S., Wollast, R., and Zhou, M.: The atmospheric input of trace species to the world ocean, Global Biogeochem. Cy., 5, 193–259, 1991.
Dutay, J. C., Bullister, J. L., Doney, S. C., Orr, J. C., Najjar, R., Caldeira, K., Campin, J. M.,

Drange, H., Follows, M., Gao, Y., Gruberi, N., Hecht, M. W., Ishida, A., Joos, F., Lindsay, K., Madec, G., Maier-Reimer, E., Marshall, J. C., Matear, R. J., Monfray, P., Mouchet, A., Plattner, G.-K., Sarmiento, J., Schlitzer, R., Slater, R., Totterdell, I. J., Weirig, M.-F., Yamanaka, Y., and Yool, A.: Evaluation of ocean model ventilation with CFC-11: comparison of 13 global ocean models, Ocean model, 4(2), 89–120, 2002.

Dutay, J. C., Jean-Baptiste, P., Campin, J. M., Ishida, A., Maier-Reimer, E., Matear, R. J., Mouchet, A., Totterdell, I. J., Yamanaka, Y., Rodgers, K., Madec, G., and Orr, J. C.: Evaluation of OCMIP-2 ocean models' deep circulation with mantle helium-3, J. Mar. Syst., 48, 15–36, 2004.

Dutay, J.-C., Lacan, F., Roy-Barman, M., and Bopp, L.: Influence of particle size and type on 231 Pa and 230 Th simulation with a global coupled biogeochemical-ocean general circulation model: A first approach, Geochem. Geophys. Geosyst., 10, Q01011, doi:10.1029/2008GC002291, 2009.

Elderfield, H.: The oceanic chemistry of the Rare Earth Elements, Phil. Trans. R. Soc. Lond., 325, 105–106, 1988.

Elderfield, H., Upstill-Goddard, R., and Sholkovitz, E. R.: The rare earth elements in rivers, estuaries, and coastal seas and their significance to the composition of ocean waters, Geochim. Cosmochim. Ac., 54, 971–991, 1990.

Fichefet, T. and Maqueda, M. A. M.: Sensitivity of a global sea ice model to the treatment of ice thermodynamics and dynamics, J. Geophys. Res.-Oceans, 102, 12609–12646, 1997.

Gehlen, M., Bopp, L., Ernprin, N., Aumont, O., Heinze, C., and Raguencau, O.: Reconciling surface ocean productivity, export fluxes and sediment composition in a global biogeochemical ocean model, Biogeosciences, 3, 521–537, 2006, http://www.biogeosciences.net/3/521/2006/.

Gent, P. R. and McWilliams, J. C.: Isopycnal Mixing In Ocean Circulation Models, J. Phys. Oceanogr., 20, 150–155, 1990.

GEOTRACES: An international study of the marine biogeochemical cycles of trace elements and isotopes, http://www.geotraces.org/, 2005.

Goldstein, S. L., O'Nions, R. K., and Hamilton, P. J.: A Sm-Nd study of atmospheric dusts and particulates from major river systems, Earth Planet. Sc. Lett., 70, 221–236, 1984.

Goldstein, S. L. and Jacobsen, S. B.: The Nd and Sr isotopic systematics of river-water dissolved material: implications for the sources of Nd and Sr in the seawater, Chem. Geol. (Isotope Geosc. Section), 66, 245–272, 1987.

Goldstein, S. L. and Hemming, S. R.: Long lived Isotopic Tracers in Oceanography, Paleoceanography, and Ice sheet dynamics, in: Treatise on Geochemistry, edited by: Elderfield, H., Elsevier Pergamon press, Amsterdam, chapter 6.17, 2003.

Greaves, M. J., Statham, P. J., and Elderfield, H.: Rare earth element mobilization from marine atmospheric dust into seawater, Mar. Chem., 46, 255–260, 1994.

Grousset, F. E., Biscaye, P. E., Zindler, A., Prospero, J., and Chester, R.: Neodymium isotopes as tracers in marine sediments and aerosols: North Atlantic, Earth Planet. Sc. Lett., 87, 367–378, 1988.

Grousset, F., Parra, M., Bory, A., Martinez, P., Bertrand, P., Shiemmield, G., and Ellam, R. M.: Saharan wind regimes traced by the Sr-Nd isotopic composition of subtropical Atlantic Sediments: last glacial maximum vs. today, Quaternary Sci. Rev., 17, 395–409, 1998.

Gutjahr, M., Frank, M., Stirling, C. H., Keigwin, L. D., and Halliday, A. N.: Tracing the Nd isotope evolution of North Atlantic deep and intermediate waters in the Western North Atlantic since the Last Glacial Maximum from Blake Ridge sediments, Earth Planet. Sc. Lett., 266, 61–77, 2008.

Henderson, G. M., Heinze, C., Anderson, R. F., and Winguth, A. M. E.: Global distribution of the Th-230 flux to ocean sediments constrained by GCM modelling, Deep-Sea Res. Pt. I, 46, 1861–1893, 1999.

Jacobsen, S. B. and Wasserburg, G. J.: Sm-Nd isotopic evolution of chondrites, Earth Planet. Sc. Lett., 50, 139–155, 1980.

Jeandel, C.: Concentration and isotopic composition of Nd in the South Atlantic Ocean, Earth Planet. Sc. Lett., 117, 581–591, 1993.

Jeandel, C., Bishop, J. K., and Zindler, A.: Exchange of Nd and its isotopes between seawater small and large particles in the Sargasso Sea, Geochim. Cosmochim. Ac., 59, 535–547, 1995.

Jeandel, C., Arsouze, T., Lacan, F., Techine, P., and Dutay, J. C.: Isotopic Nd compositions and concentrations of the lithogenic inputs into the ocean: A compilation, with an emphasis on the margins, Chem. Geol., 239, 156–164, 2007.

Johannesson, K. H. and Burdige, D. J.: Balancing the global oceanic neodymium budget: Evaluating the role of groundwater, Earth Planet. Sc. Lett., 253, 129–142, 2007.

Jones, K., Khatiwala, S., Goldstein, S. L., Hemming, S. R., and Van de Flierdt, T.: Modeling the distribution of Nd isotopes in the oceans using an offline Ocean General Circulation Model, Earth Planet. Sc. Lett., 202(3–4), 610–619, 2008.

Khatiwala, S., Visbeck, M., and Cane, M. A.: Accelerated simulation of passive tracers in ocean circulation models, Ocean Model, 9, 51–69, 2005.
Kriest, I.: Different parameterizations of marine snow in a 1-D-model and their influence on representation of marine snow, nitrogen budget and sedimentation, Deep-Sea Res. Pt. I, 49, 2133–2162, 2002.
Lacan, F. and Jeandel, C.: Tracing Papua New Guinea imprint on the central Equatorial Pacific Ocean using neodymium isotopic compositions and Rare Earth Element patterns, Earth Planet. Sc. Lett., 186, 497–512, 2001.
Lacan, F. and Jeandel, C.: Subpolar Mode Water formation traced by neodymium isotopic composition. Geophys. Res. Lett., 31, L14306, doi:10.1029/2004GL019747, 2004,
Lacan, F. and Jeandel, C.: Neodymium isotopes as a new tool for quantifying exchange fluxes at the continent – ocean interface, Earth Planet. Sc. Lett., 232, 245–257, 2005.
Madec, G.: NEMO ocean engine, Note du Pole de modélisation, Institut Pierre-Simon Laplace (IPSL), 27, ISSN No 1288-1619, 2008.
Monod, J.: Recherches sur la croissance des cultures bactériennes, Hermann, Paris, 1942.
Milliman, J. D. and Syvitski, J. P. M.: Geomorphic/tectonic control of sediment discharge to the ocean: the importance of small mountain rivers, J. Geol., 100, 325–344, 1992.
Nozaki, Y., Horibe, Y., and Tsubota, H.: The water column distribution of thorium isotopes in the western North Pacific, Earth Planet. Sc. Lett., 54, 203–216, 1981.
Nozaki, Y. and Zhang, J.: The rare earth elements and yttrium in the coastal/offshore mixing zone of Tokyo Bay waters and Kuroshio, Biogeochemical Processes and Ocean Flux in the Western Pacific, edited by: Sakai, H. and Nozaki, Y., 171–184, 1995.
Nozaki, Y. and Alibo, D.: Importance of vertical geochemical processes in controlling the oceanic profiles of dissolved rare earth elements in the northeastern Indian Ocean, Earth Planet. Sc. Lett., 205, 155–172, 2003.
Oka, A., Kato, S., and Hasumi, H.: Evaluating effect of ballast mineral on deep-ocean nutrient concentration by using an ocean general circulation model, Global Biogeochem. Cy., 22, 3, GB3004, doi:10.1029/2007GB003067, 2008.
Piepgras, D. J., Wasserburg, G. J., and Dasch, E. G.: The isotopic composition of Nd in different ocean masses, Earth Planet. Sc. Lett., 45, 223–236, 1979.
Piepgras, D. J. and Wasserburg, G. J.: Neodymium isotopic variations in seawater, Earth Planet. Sc. Lett., 50, 128–138, 1980.
Piepgras, D. J. and Wasserburg, G. J.: Isotopic composition of neodymium in waters from the

Drake Passage, Science, 217, 207–217, 1982.
Piepgras, D. J. and Wasserburg, G. J.: Influence of the Mediterranean outflow on the isotopic composition of neodymium in waters of the North Atlantic, J. Geophys. Res., 88, 5997–6006, 1983.
Piepgras, D. J. and Wasserburg, G. J.: Rare earth element transport in the western North Atlantic inferred from isotopic observations, Geochim. Cosmochim. Ac., 51, 1257–1271, 1987.
Piotrowski, A. M., Goldstein, S. L., Hemming, S. R., and Fairbanks, R. G.: Intensification and variability of ocean thermohaline circulation through the last deglaciation, Earth Planet. Sc. Lett., 225, 205–220, 2004.
Rutberg, R. L., Hemming, S. R., and Goldstein, S. L.: Reduced North Atlantic deep Water flux to the glacial Southern Ocean inferred from neodymium isotope ratios, Nature, 405, 935–938, 2000.
Shimizu, H., Tachikawa, K., Masuda, A., and Nozaki, Y.: Cerium and neodymium ratios and REE patterns in seawater from the North Pacific Ocean, Geochim. Cosmochim. Ac., 58, 323–333, 1994.
Sholkovitz, E., Landing, W., and Lewis, B.: Ocean particle chemistry: The fractionation of Rare Earth Elements between suspended particles and seawater, Geochim. Cosmochim. Ac., 58, 1567–1579, 1994.
Sholkovitz, E. R.: The geochemistry of rare earth elements in the Amazon River estuary, Geochim. Cosmochim. Ac., 57, 2181–2190, 1993.
Siddall, M., Henderson, G. M., Edwards, N. R., Frank, M., Müller, S. A., Stocker, T. F., and Joos, F.: Pa-231/Th-210 fractionation by ocean transport, biogenic particle flux and particle type, Earth Planet. Sc. Lett., 237, 135–155, 2005.
Siddall, M., Khatiwala, S., Van de Flierdt, T., Jones, K., Goldstein, S. L., Hemming, S. R., and Anderson, R. F.: Towards explaining the Nd paradox using reversible scavenging and the Transport Matrix Method, Earth Planet. Sc. Lett., 274, 448–461, 2008.
Tachikawa, K., Jeandel, C., and Dupré, B.: Distribution of rare earth elements and neodymium isotopes in settling particulate material of the tropical Atlantic Ocean (EUMELI site), Deep-Sea Res., 44, 1769–1792, 1997.
Tachikawa, K., Jeandel, C., and Roy-Barman, M.: A new approach to Nd residence time in the ocean: the role of atmospheric inputs, Earth Planet. Sc. Lett., 170, 433–446, 1999.
Tachikawa, K., Athias, V., and Jeandel, C.: Neodymium budget in the ocean and paleoceanographic implications, J. Geophys. Res., 108, 3254, doi:3210.1029/1999JC000285, 2003.

Tegen, I. and Fung, I.: Contribution to the atmospheric mineral aerosol load from land surface modification, J. Geophys. Res., 100, 18707–18726, 1995.
Timmermann, R., Goosse, H., Madec, G., Fichefet, T., Ethe, C., and Duliere, V.: On the representation of high latitude processes in the ORCA-LIM global coupled sea ice-ocean model, Ocean Model, 8, 175–201, 2005.
Van De Flierdt, T., Frank, M., Lee, D. C., Halliday, A. N., Reynolds, B. C., and Hein, J. R.: New constraints on the sources and behavior of neodymium and hafnium in seawater from Pacific Ocean ferromanganese crusts, Geochim. Cosmochim. Ac., 68, 3827–3843, 2004.
von Blanckenburg, F., O'Nions, P. K., Belshaw, N. S., Gibb, A., and Hein, J. R.: Global distribution of beryllium isotopes in deep ocean water as derived from Fe-Mn crusts, Earth Planet. Sc. Lett., 141, 213–226, 1996.
von Blanckenburg, F.: Perspectives: Paleoceanography – Tracing past ocean circulation?, Science, 286, 1862–1863, 1999.
Zhang, Y., Lacan, F., and Jeandel, C.: Dissolved rare earth elements tracing lithogenic inputs over the Kerguelen Plateau (Southern Ocean), Deep-Sea Res. Pt. II, 55, 638–652, 2008.

Table 1. Main characteristics of equilibrium partition coefficients and source fluxes for each experiment. Residence time of Nd in the ocean is calculated using the sum of flux (source or sink) and the total quantity of Nd simulated in the ocean: $\tau = Q_{Nd}/(S(A_T)_{sed} + S(A_T)_{surf})$.

Experience	Global flux of BE $(S(A_T)_{sed})$ in g(Nd)/yr	Equilibrium partition coefficient					Residence time (τ in years)	Total quantity of oceanic Nd (Q_{Nd} in g(Nd))
		K_{POMs}	K_{POMb}	K_{BSi}	K_{CaCO_3}	K_{litho}		
EXP1	0	1.4×10^{7}	0	0	0	2.3×10^{6}	760	4.1×10^{11}
EXP2	8×10^{9}	1.4×10^{7}	0	0	0	2.3×10^{6}	640	5.3×10^{12}
EXP3	8×10^{9}	7.7×10^{7}	0	0	0	2.3×10^{6}	150	1.3×10^{12}
EXP4	8×10^{9}	1.4×10^{7}	2.6×10^{5}	1.8×10^{5}	7.8×10^{5}	2.3×10^{6}	125	1.1×10^{12}
EXP5	1.1×10^{9}	1.4×10^{7}	5.2×10^{4}	3.6×10^{4}	1.6×10^{5}	4.6×10^{5}	360	4.2×10^{12}

BGD
6, 5549–5588, 2009

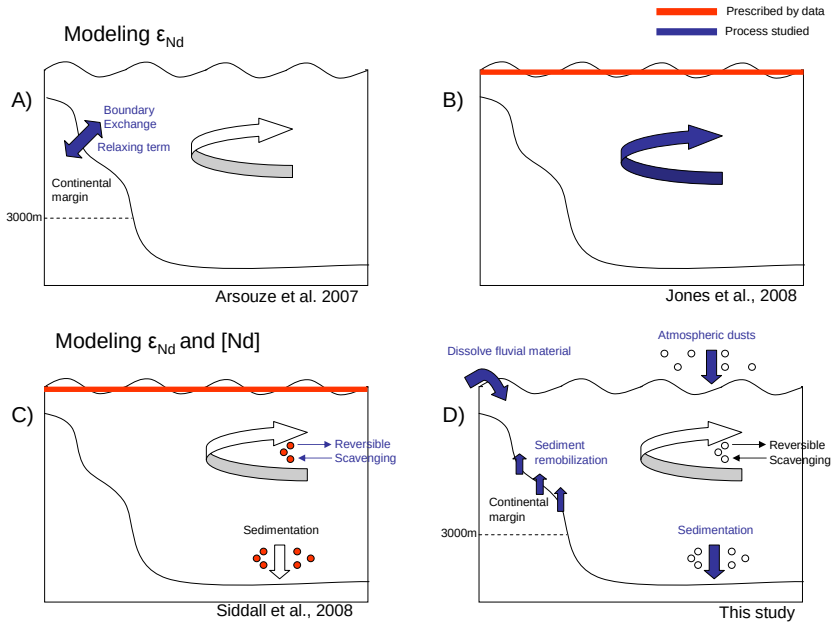

Fig. 1. Summary of the main Nd oceanic modelling efforts already published and using an OGCM. In each case, the different processes explicitly simulated are represented. Arrows and legends in blue underline the processes specifically studied, while red components refer to parameters prescribed by the data. **(A)** Arsouze et al. (2007), modelling only Nd IC, focused on the role of Boundary Exchange using a relaxing term and defined on the first 3000 m of the continental margin: this work evidenced the importance of this process in the element's global cycle. **(B)** Jones et al. (2008), prescribing a surface ε_{Nd} value estimated by the data suggested that Nd IC distribution can simply be explained by water mass mixing, except in the North Pacific region, where some external radiogenic inputs are required. **(C)** Using prescribed surface ε_{Nd} and Nd concentration, as well as particles fields determined by satellite observations and then interpolated within the water column, Siddall et al. (2008) evidenced the major role of vertical cycling (reversible scavenging process) to reproduce both ε_{Nd} and Nd concentration oceanic distribution. **(D)** In this study, besides confirming, as in Siddall et al. (2008), the role of vertical cycling in Nd oceanic distribution, we aimed to determine and quantify the different sources involved in the Nd oceanic cycle. The Boundary Exchange process is implicitly taken into account via sediment redissolution along the continental margins (source term) as well as by particle sedimentation (sink term).

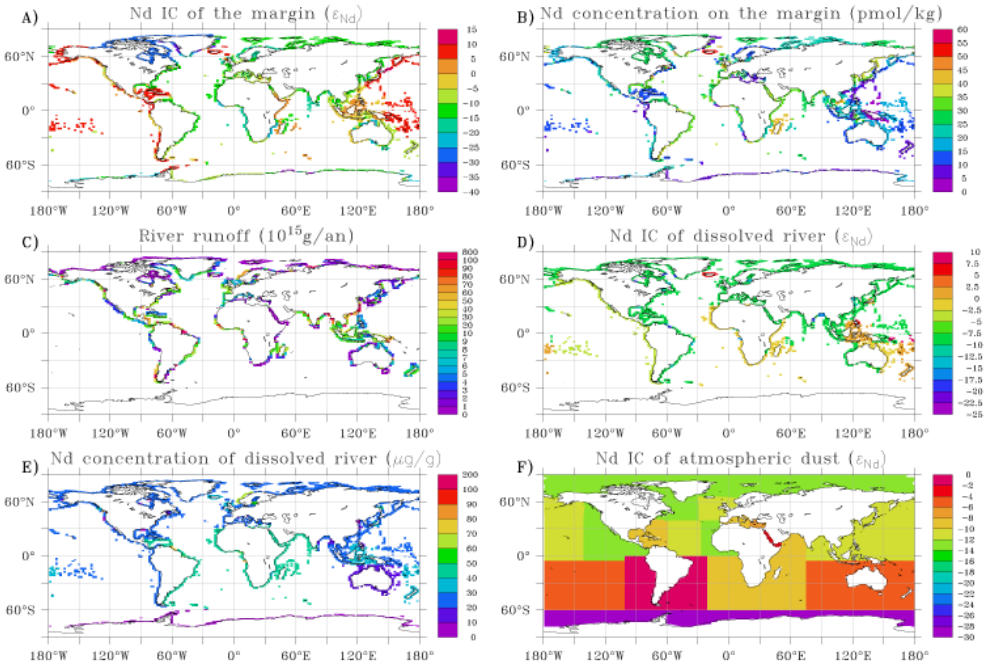

Fig. 2. Input maps applied to the model. **(A)** ε_{Nd} map along the continental margin determined by Jeandel et al. (2007). This input is applied to the sedimentary remobilization source F_{sed}. **(B)** Nd concentration map along continental margin (in μg/g) determined by Jeandel et al. (2007). This input is also applied to the sedimentary remobilization source F_{sed}. **(C)** Runoff map prescribed by NEMO OGCM (in 10^{15} g/yr). Scale is non linear. **(D)** ε_{Nd} map of river runoff given by Goldstein and Jacobsen (1987). **(E)** Nd concentration of river runoff (in ng/g) Goldstein and Jacobsen (1987); scale is non linear. **(F)** Interpolated ε_{Nd} map of atmospheric dust (Grousset et al., 1988, 1998; Jeandel et al., 2007). Dust particle fields are provided by Tegen and Fung (1995), and Nd concentration is set constant to 20 μg/g.

BGD
6, 5549–5588, 2009

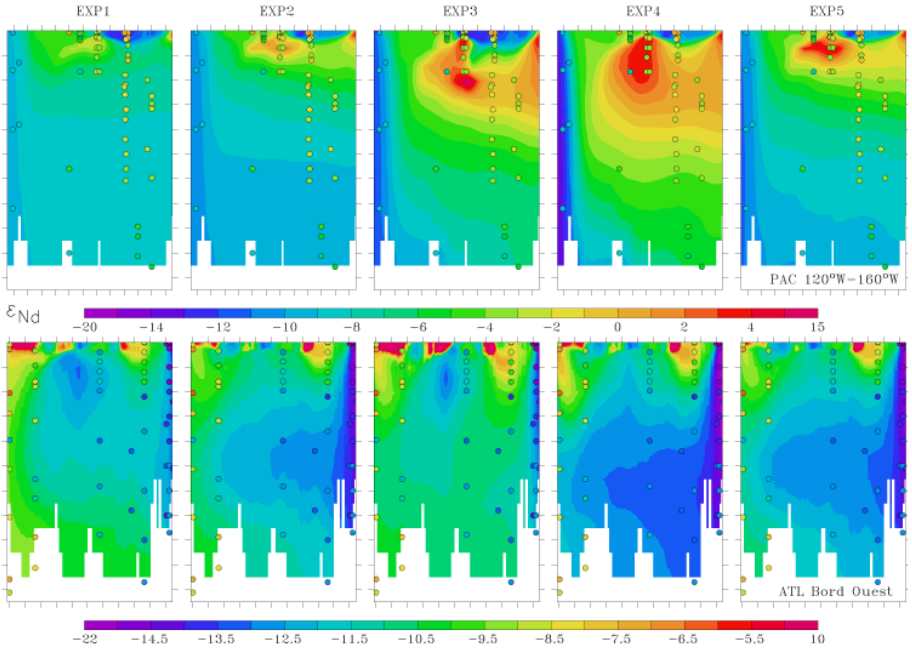

Fig. 3. Vertical ε_{Nd} sections for all simulations, in the Pacific basin averaged between 120° W and 160° W (upper panel), and along the western section of the Atlantic basin (lower panel). Superimposed circles are the data. Colour scales are the same for all simulations and data, but different for each section. Main characteristics for each experiment are summarized in Table 1.

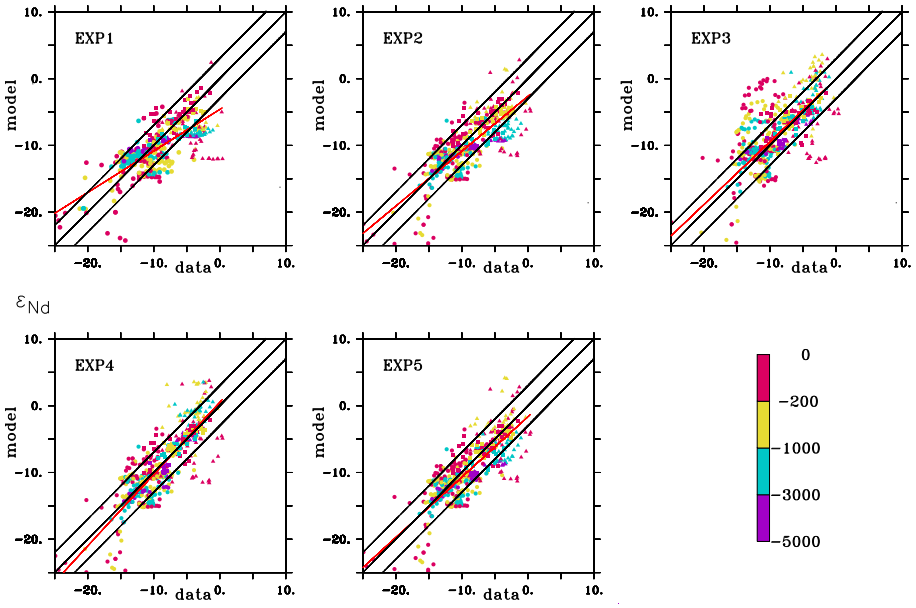

Fig. 4. ε_{Nd} model/data cross plot for each experiment as a function of depth (colour code). Circles represent the data located in the Atlantic basin; squares are data in the Indian basin and triangles are data in the Pacific basin. Red line is the linear interpolation line. Black lines represent the lines ε_{Nd} (model)=ε_{Nd} (data) and ε_{Nd} (model)=ε_{Nd} (data)±3 ε_{Nd}. Main characteristics for each experiment are summarized in Table 1.

BGD
6, 5549–5588, 2009

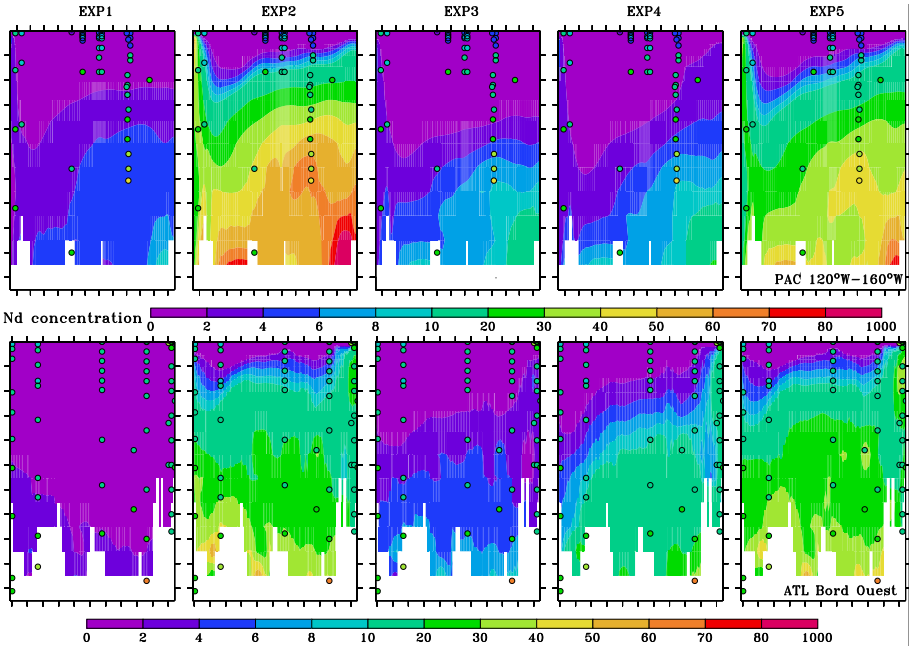

Fig. 5. Same figure as Fig. 3, for Nd concentration (in pmol/kg).

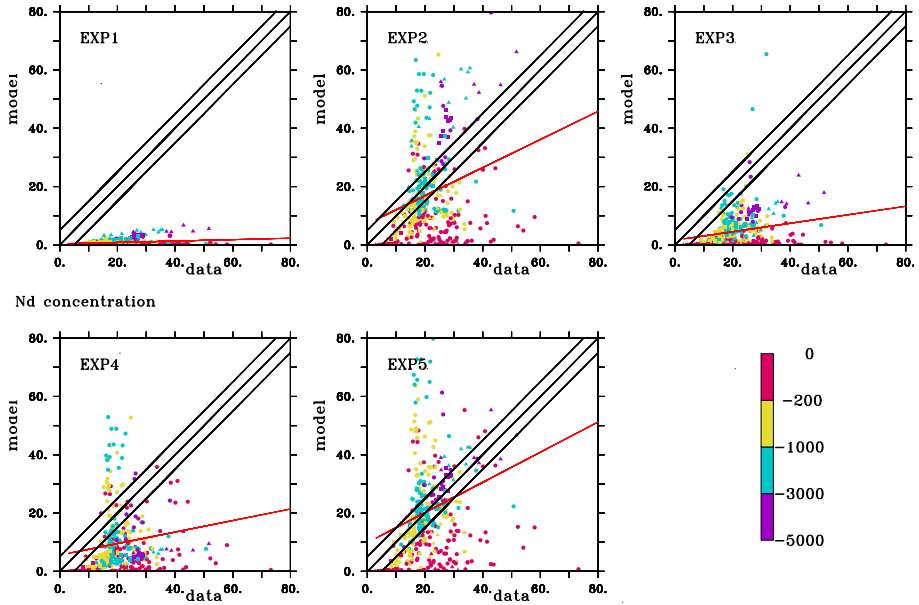

Fig. 6. Same figure as Fig. 4, for Nd concentration (in pmol/kg). Black lines represent the lines [Nd] (model)=[Nd] (data) and [Nd] (model)=[Nd] (data)±10 pmol/kg.

BGD
6, 5549–5588, 2009

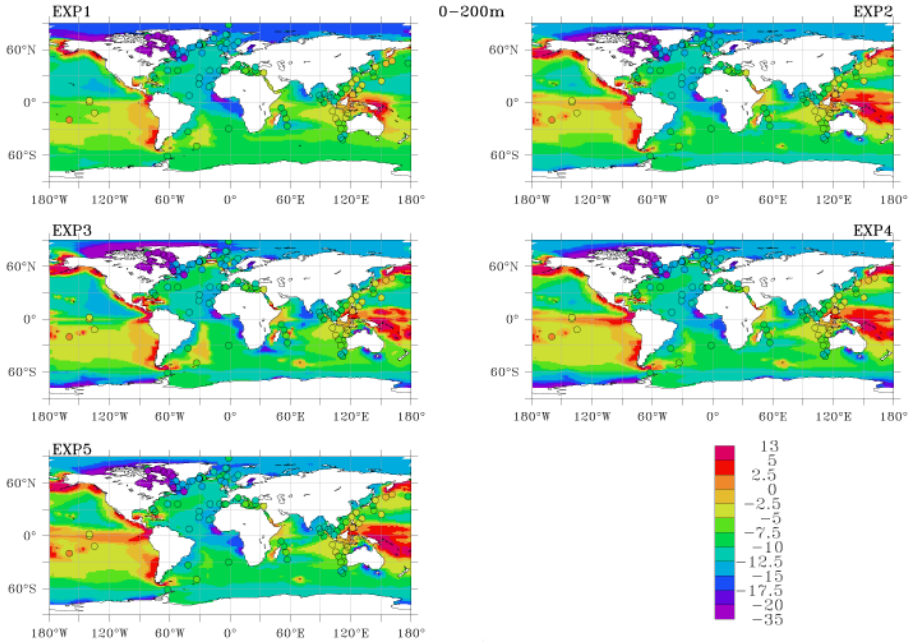

Fig. 7. Horizontal ε_{Nd} maps averaged between 0 and 200 m, for all the experiments. Superimposed circles represent the data at the same depth. Colour scale is non linear. Main characteristics for each experiment are summarized in Table 1.

BGD
6, 5549–5588, 2009

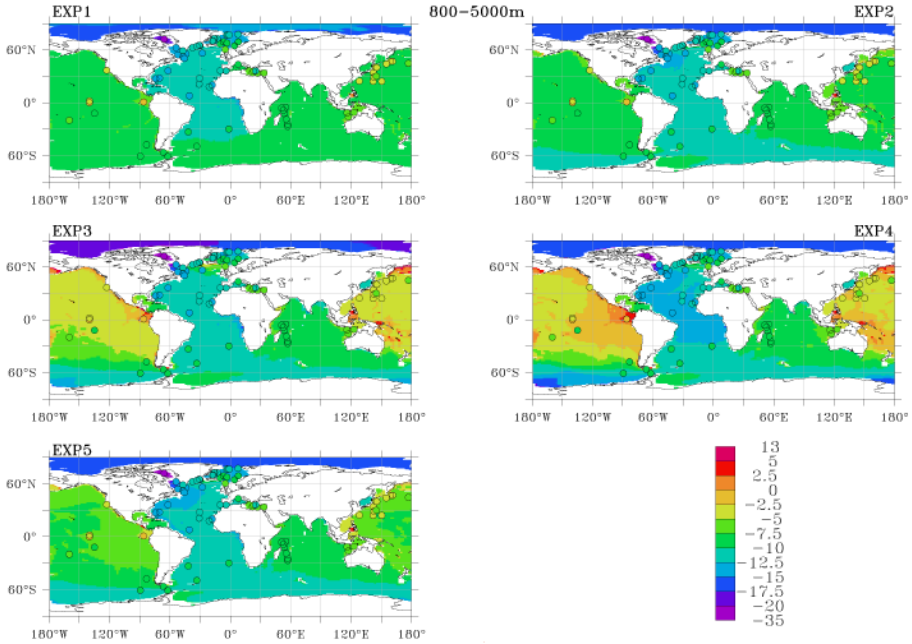

Fig. 8. Same figure as Fig. 7, with ε_{Nd} averaged between 800 and 5000 m.

BGD
6, 5549–5588, 2009

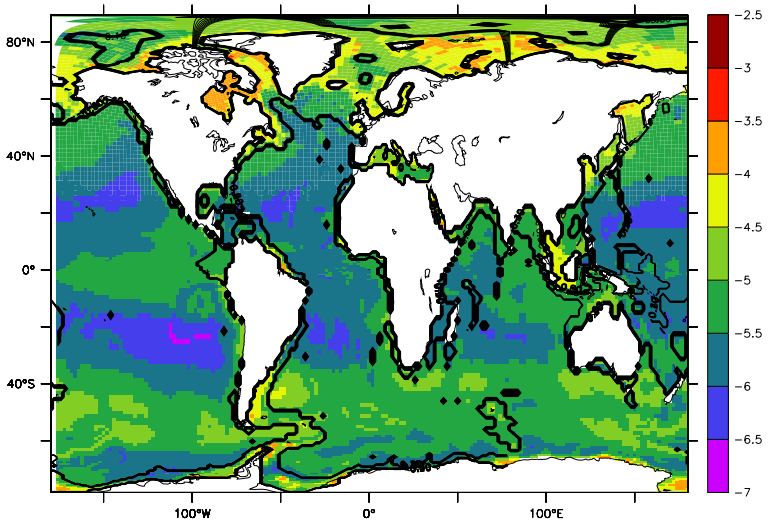

Fig. 9. Logarithmic map of Nd flux to the seafloor for experience EXP5, in $g/m^{-2}/yr^{-1}$. Black line delimitates the continental margin area, where 64% of the Nd sink is located.

BGD
6, 5549–5588, 2009